

Critical Level Statistics and Anomalous Localized States at the Anderson Transition

H. Obuse and K. Yakubo

Department of Applied Physics, Graduate School of Engineering, Hokkaido University, Sapporo 060-8628, Japan.

We study the level-spacing distribution function $P(s)$ at the Anderson transition by paying attention to anomalously localized states (ALS) which contribute to statistical properties at the critical point. It is found that the distribution $P(s)$ for level pairs of ALS coincides with that for pairs of typical multifractal states. This implies that ALS do not affect the shape of the critical level-spacing distribution function. We also show that the insensitivity of $P(s)$ to ALS is a consequence of multifractality in tail structures of ALS.

PACS numbers: 71.30.+h, 73.20.Fz, 64.60.Ak, 71.70.Ej

I. INTRODUCTION

It is well recognized that a statistical description of spectral correlations provides a powerful tool to study the disorder induced metal-insulator transition, namely, the Anderson transition.^{1,2,3,4} Among several measures representing spectral correlations, the nearest-neighbor level-spacing distribution function $P(s)$ has been extensively studied so far, where s is the energy spacing between adjacent levels normalized by the mean level spacing Δ . The functional form of $P(s)$ is closely related to the localization nature of corresponding wavefunctions. According to the random matrix theory,⁵ the level-spacing distribution function in the metallic phase is approximated by the Wigner-Dyson distribution, namely,

$$P_W(s) = a_\beta s^\beta \exp(-c_\beta s^2), \quad (1)$$

where β ($= 1, 2$, and 4 for the orthogonal, the unitary, and the symplectic ensembles, respectively) characterizes the universality classes. The coefficients a_β and c_β are determined by the normalization conditions $\int P_W(s)ds = \int sP_W(s)ds = 1$, as $a_1 = \pi/2$, $a_2 = 32/\pi^2$, $a_4 = 2^{18}/3^6\pi^3$, $c_1 = \pi/4$, $c_2 = 4/\pi$, and $c_4 = 64/9\pi$. For $s \ll 1$, the distribution function is proportional to s^β , which implies that adjacent energy levels cannot approach each other indefinitely because of mixing between two extended states. Since $P_W(s) \propto s^4$ for $s \ll 1$ for the symplectic ensemble, the level repulsion in this ensemble is strongest amongst the three classes. In the insulating regime, mixing of quantum states belonging to adjacent levels can be ignored and the energy levels are uncorrelated. Consequently, the level-spacing distribution function obeys the Poissonian,

$$P_P(s) = \exp(-s). \quad (2)$$

The Poisson distribution for the insulating phase and the three kinds of Wigner-Dyson distribution functions for the metallic phase have been confirmed numerically in two and three dimensions.^{6,7}

In addition to these two types of distribution functions, there exists the third distribution at the critical point of the Anderson transition.^{4,8,9,10,11,12} A critical wavefunction percolates over the whole system in a multifractal

manner reflecting no characteristic length scales, and the spatial profile of the wavefunction is similar to neither extended nor localized states.^{13,14,15} Since the level statistics are governed by wavefunction profiles,¹⁶ the critical level statistics are expected to be different from both P_W and P_P . In fact, it has been numerically elucidated that the critical level-spacing distribution cannot be expressed by either Eq. (1) or (2) and is scale independent and universal. The analytical form of the critical distribution $P(s)$ is of great interest.

There exist attempts to solve this problem in a framework of the random matrix theory. In the random matrix theory, a matrix ensemble is characterized by the joint probability distribution of eigenvalues $\{\varepsilon_i\}$. This probability distribution can be regarded as the Gibbs function of one-dimensional interacting fictitious particles at the inverse temperature β ($= 1, 2, 4$), whose positions are given by ε_i . If these particles interact each other via a logarithmic repulsion, namely, $V_{\text{int}}(|\varepsilon_i - \varepsilon_j|) = -\ln|\varepsilon_i - \varepsilon_j|$ and are in the confinement potential $V_{\text{pot}}(\varepsilon_i) = \varepsilon_i^2$, the Gibbs function gives the Wigner-Dyson level spacing distribution functions Eq. (1). In order to obtain the analytical form of $P(s)$ at criticality, two types of ingenuities have been proposed. One is to set the power-law interaction $V_{\text{int}}(|\varepsilon_i - \varepsilon_j|) \propto |\varepsilon_i - \varepsilon_j|^{-\gamma}$ in the Gibbs function, where $\gamma = 1 - 1/d\nu$ and ν is the localization length exponent.^{17,18} This leads the critical distribution function proportional to $\exp(-c'_\beta s^{1+1/d\nu})$ for $s \gg 1$. The whole profile of $P(s)$ is then conjectured to be

$$P(s) = a'_\beta s^\beta \exp(-c'_\beta s^{1+1/d\nu}). \quad (3)$$

However, most of numerical results presented so far deviate from this analytical form.^{19,20,21,22,23} Although $P(s)$ for $s \ll 1$ is proportional to s^β , $P(s)$ obtained by numerical studies behaves as $\exp(-s/s_0)$ with $s_0 < 1$ in the large s limit. Another attempt is to construct a random-matrix ensemble with a log-squared potential $V_{\text{pot}}(\varepsilon_i) = (\ln \varepsilon_i)^2/2a$.^{24,25} Using such a non-Gaussian random-matrix ensemble, Nishigaki has obtained a differential equation for the critical distribution $P(s)$.²⁵ Although the numerical solution of this differential equation well reproduces the critical distribution $P(s)$ calculated by exact diagonalizations, the theory contains an ambiguous parameter a and the closed form of $P(s)$ remains to

be unknown. Thus the analytical form of $P(s)$ at the Anderson transition is still unclear.

These arguments on $P(s)$ are based on the assumption that all of critical states are multifractal characterized by an entire spectrum comprising infinitely many exponents. Recently, it has, however, been shown²⁶ that anomalously localized states (ALS)^{27,28,29,30,31,32,33} in which most of amplitudes concentrate on a narrow spatial region exist *with a finite probability in infinite systems* at the Anderson transition point. ALS are brought by statistical fluctuations in disorder realizations and show no multifractality because of the characteristic length of large amplitude regions. It should be noted that typical states are kept to be multifractal in critical systems. When studying statistical properties of physical quantities defined at the critical point, one should take notice of the influence of ALS.³⁴ In particular, ALS make a significant contribution to distribution functions of critical quantities. If the level-spacing distribution $P(s)$ calculated at the critical point is strongly affected by ALS, there is a possibility that $P(s)$ for level pairs of typical wavefunctions might be totally different from that obtained numerically so far. It follows that the contribution of ALS should be eliminated from a simulation result for checking numerically the validity of an analytical expression of $P(s)$ at criticality. This is because previous theoretical arguments are essentially based on the random matrix theory which does not allow the existence of ALS.

In this paper, we study numerically the influence of ALS to the level-spacing distribution function at the Anderson transition. Energy levels and their corresponding wavefunctions at the critical point are prepared in two-dimensional symplectic systems described by the SU(2) model.³⁵ By employing our recently proposed definition of ALS at criticality, we distinguish ALS from typical multifractal states (MS) and construct ALS (MS) level-pair ensembles which contains only pairs of energy levels corresponding to ALS (MS). It is found that the critical level-spacing distribution function for an ALS level-pairs ensemble coincides with that for MS level-pair ensembles and for the entire ensemble. All characteristics in level-pair ensembles are absorbed by their mean level spacings. This implies that the elimination of ALS does not affect the profile of the level-spacing distribution function. We also show that this remarkable feature of $P(s)$ is a consequence of multifractality in tail structures of ALS. This paper is organized as follows. In Sec. II, we give a quantitative definition of ALS at the critical point based on the idea that ALS do not show multifractality. Level-pair ensembles constructed for extracting contributions of ALS are also defined in this section. Furthermore, a brief explanation of the SU(2) model employed in this paper is given here. Calculated results are shown in Sec. III. An interpretation of our results and a condition that the critical level-spacing distribution function should satisfy are presented in Sec. IV, together with our conclusions.

II. DEFINITION OF ANOMALOUSLY LOCALIZED STATES AND THE MODEL

In order to study the influence of ALS to the critical level-spacing distribution function, it is necessary to distinguish ALS from a set of critical wavefunctions. To this end, we employ an expedient definition of ALS proposed in Ref. 18, which is based on the fact that a typical critical wavefunction is multifractal while ALS are not. Multifractal distributions of wavefunction amplitudes can be characterized by the box-measure correlation function $G_q(l, L, r)$,³⁶

$$G_q(l, L, r) = \frac{1}{N_b N_{b_r}} \sum_b \sum_{b_r} \mu_{b(l)}^q \mu_{b_r(l)}^q, \quad (4)$$

where $\mu_{b(l)} = \sum_{i \in b(l)} |\psi_i|^2$ and $\mu_{b_r(l)} = \sum_{i \in b_r(l)} |\psi_i|^2$ are the box measures of squared amplitudes of a wavefunction $|\psi_i|^2$ in a box $b(l)$ of size l and in a box $b_r(l)$ of size l fixed distance $r - l$ away from the box $b(l)$, respectively, N_b (or N_{b_r}) is the number of boxes $b(l)$ [or $b_r(l)$], q is the moment, and the summations are taken over all such boxes in a system of size L . We concentrate on the l dependence of $G_2(l, L, r)$ for $r = l$ and the r dependence of $G_2(l, L, r)$ for $l = 1$. Denoting $Q(l) \equiv G_2(l, L, r = l)$ and $R(r) \equiv G_2(l = 1, L, r)$, these two functions obey, if the wavefunction is multifractal, the following power laws,³⁶

$$Q(l) \propto l^{d+\tau(4)}, \quad (5)$$

and

$$R(r) \propto r^{-[d+2\tau(2)-\tau(4)]}, \quad (6)$$

where d and $\tau(q)$ are the spatial dimension and the mass exponent for the q th moment of measures, respectively.¹⁵

We regard wavefunctions not satisfying Eqs. (5) and (6) as ALS at the critical point. To make this definition quantitative, we introduce variances $\text{Var}(\log_{10} Q)$ and $\text{Var}(\log_{10} R)$ from functions $\log_{10} Q(l) = [d + \tau(4)] \log_{10} l + c_Q$ and $\log_{10} R(r) = -[d + 2\tau(2) - \tau(4)] \log_{10} r + c_R$ obtained by the least-square fit for a specific wavefunction. Non-multifractality of the wavefunction is quantified by

$$\Gamma = \lambda \text{Var}(\log_{10} Q) + \text{Var}(\log_{10} R), \quad (7)$$

where λ is a factor to compensate the difference between average values of $\text{Var}(\log_{10} Q)$ and $\text{Var}(\log_{10} R)$. The quantity Γ is small (large) when a given wavefunction is close to (far from) the typical multifractal state. We call Γ the atypicality of the wavefunction. Thus one can expediently regard the wavefunctions with $\Gamma > \Gamma_{\text{ALS}}^*$ and $\Gamma < \Gamma_{\text{MS}}^*$ as ALS and MS, respectively, where Γ_{ALS}^* and Γ_{MS}^* are critical values of Γ for ALS and MS.

Our aim is to calculate level-spacing distribution functions for ALS and MS level-pair ensembles. The ALS level-pair ensemble S_{ALS} (the MS level-pair ensemble

S_{MS}) is defined as a set of pairs of adjacent levels whose corresponding wavefunctions are both ALS (MS), namely,

$$S_{\text{ALS}}(\Gamma_{\text{ALS}}^*) = \{(\varepsilon, \varepsilon') : \Gamma > \Gamma_{\text{ALS}}^* \text{ and } \Gamma' > \Gamma_{\text{ALS}}^*\}, \quad (8)$$

and

$$S_{\text{MS}}(\Gamma_{\text{MS}}^*) = \{(\varepsilon, \varepsilon') : \Gamma < \Gamma_{\text{MS}}^* \text{ and } \Gamma' < \Gamma_{\text{MS}}^*\}, \quad (9)$$

where ε and ε' are adjacent energy levels in the critical region and Γ and Γ' are the atypicalities of wavefunctions belonging to ε and ε' , respectively. In addition to S_{ALS} and S_{MS} , the ensemble of the whole pairs of adjacent levels in the critical region is denoted by S_0 , which is called the entire ensemble or the original ensemble.

In the present paper, level-spacing distribution functions are calculated for critical states in two-dimensional electron systems with strong spin-orbit interactions (symplectic systems) because of the advantage of system sizes. Among several models belonging to this universality class, we adopt the SU(2) model,³⁵ because scaling collections are known to be negligible due to a very short spin-relaxation length. The Hamiltonian is compactly written in a quaternion form as

$$\mathbf{H} = \sum_i \epsilon_i \mathbf{c}_i^\dagger \mathbf{c}_i - V \sum_{i,j} \mathbf{R}_{ij} \mathbf{c}_i^\dagger \mathbf{c}_j, \quad (10)$$

where \mathbf{c}_i^\dagger (\mathbf{c}_i) is the creation (annihilation) operator acting on a quaternion state vector³⁷ and ϵ_i represents the on-site random potential distributed uniformly in the interval $[-W/2, W/2]$. (Quaternion-real quantities are denoted by bold symbols.) The strength of the hopping V is taken to be the unit of energy. The quaternion-real hopping matrix element \mathbf{R}_{ij} between the sites i and j is given by

$$\begin{aligned} \mathbf{R}_{ij} = & \cos \alpha_{ij} \cos \beta_{ij} \boldsymbol{\tau}^0 + \sin \gamma_{ij} \sin \beta_{ij} \boldsymbol{\tau}^1 \\ & - \cos \gamma_{ij} \sin \beta_{ij} \boldsymbol{\tau}^2 + \sin \alpha_{ij} \cos \beta_{ij} \boldsymbol{\tau}^3, \end{aligned} \quad (11)$$

for the nearest neighbor sites i and j , and $\mathbf{R}_{ij} = 0$ for otherwise. $\boldsymbol{\tau}^\mu$ ($\mu = 0, 1, 2, 3$) is the primitive elements of the quaternion algebra. Random quantities α_{ij} and γ_{ij} are distributed uniformly in the range of $[0, 2\pi)$, and β_{ij} is distributed according to the probability density $P(\beta)d\beta = \sin(2\beta)d\beta$ for $0 \leq \beta \leq \pi/2$. The critical disorder W_c of this model is known to be 5.952 for the energy $E = 1.0$.³⁵

III. RESULTS

We calculate the level-spacing distribution functions $P(s)$ for ALS and MS level-pair ensembles at the metal-insulator transition point of the two-dimensional SU(2) model. Periodic boundary conditions are imposed in the both directions of systems of size $L = 36$. The number of disorder realizations is 2×10^5 . We extract three successive eigenenergies from one sample with $W = 5.952$,

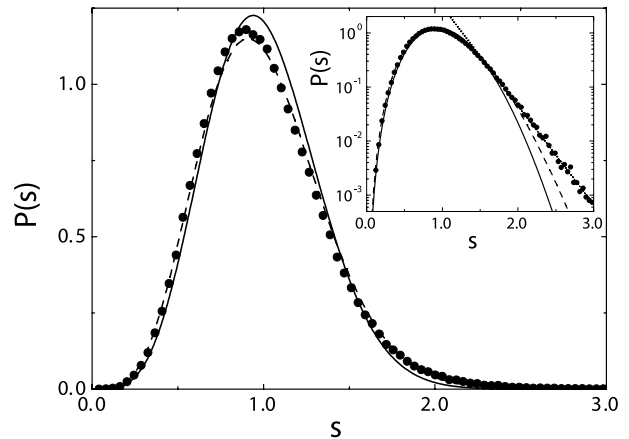


FIG. 1: Critical level-spacing distribution function for the entire level-pair ensemble S_0 (circles). Solid and dashed lines represent the Wigner-Dyson distribution function for the symplectic class ($\beta = 4$) and the critical distribution predicted by Aronov *et al.*,¹⁷ namely, Eq. (3) with $\nu = 0.75$. The inset shows the same plots in a semilogarithmic scale. Dotted line showing an exponential decay is a guide to the eye.

which are closest to the critical energy $E = 1.0$. The total number of level spacings is then 4×10^5 . All of these level spacings construct the entire level-pair ensemble S_0 . In contrast to conventional studies of the level statistics, eigenstates are also required for distinguishing ALS and MS from the set of critical states. The forced oscillator method^{38,39} for quaternion-real matrices has been employed to calculate unfolded eigenvalues and the corresponding eigenvectors.

Figure 1 shows the level-spacing distribution $P(s)$ for the entire level-pair ensemble S_0 . The function $P(s)$ is proportional to s^4 for $s \ll 1$, while it is slightly shifted toward smaller s as compared with the Wigner-Dyson distribution. In the limit of $s \gg 1$, $P(s)$ seems to decay exponentially as seen in the inset of Fig. 1. These features of $P(s)$ are consistent with numerical results reported previously.^{19,20,21} In fact, when we try to fit our data of $P(s)$ to the critical distribution function predicted by Aronov *et al.*,¹⁷ the exponent ν in Eq. (3) is found to be 0.75. This value is very close to that obtained previously by a similar analysis for the Ando model⁴⁰ as an alternative model of the two-dimensional symplectic system,²¹ though it largely deviates from the value believed to be correct for this universality class ($\nu = 2.8$). This implies that previous numerical results with large energy windows correctly represent the level-spacing distribution at criticality, which differs from Eq. (3) at large s values but behaves exponentially.

We have prepared several level-pair ensembles S_{ALS} and S_{MS} by choosing values of Γ_{ALS}^* and Γ_{MS}^* to calculate the level-spacing distributions for these ensembles. The parameter λ in the definition of Γ [see Eq. (7)] is set to be 3.0, because the average of $\text{Var}(\log_{10} R)$ is about three times larger than that of $\text{Var}(\log_{10} Q)$, while the choice

TABLE I: List of the level-pair ensembles employed in the present work. The ensemble S_0 is the entire (original) ensemble. The quantity Γ^* represents Γ_{ALS}^* for ALS ensembles and Γ_{MS}^* for MS ones. Δ is the mean level spacing of each ensemble, and N is the number of level pairs included in the ensemble.

Ensemble	ALS Ensemble				MS Ensemble		
	S_0	S_{ALS}^1	S_{ALS}^2	S_{ALS}^3	S_{MS}^1	S_{MS}^2	S_{MS}^3
Γ^*	—	0.03	0.025	0.01	0.01	0.015	0.03
$\Delta (\times 10^{-4})$	8.12	7.68	7.74	7.99	8.39	8.33	8.22
N	400 000	39 100	59 154	226 802	32 881	82 172	227 421

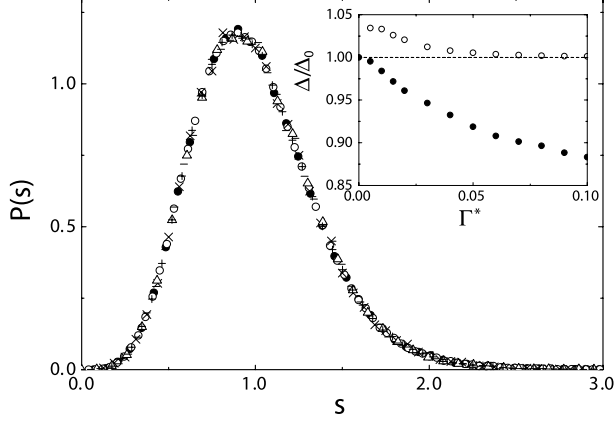


FIG. 2: Critical level-spacing distribution functions for ALS and MS level-pair ensembles. Symbols Δ , $-$, \times , $+$, and \circ represent $P(s)$ for level-pair ensembles S_{ALS}^1 , S_{ALS}^2 , S_{MS}^1 , S_{MS}^2 , and S_0 , respectively. Filled circles show $P(s)$ for the mixed level-pair ensemble S_{mix} with $\Gamma^* = 0.01$. The inset exhibits the mean level spacings for ALS level-pair ensembles (filled circles) and MS ensembles (open circles) rescaled by the mean spacing Δ_0 for S_0 . The abscissa indicates Γ_{ALS}^* for filled circles and Γ_{MS}^* for open circles.

of λ does not affect our conclusions. Statistical data of seven ensembles used in the present work is listed in Table I.

Figure 2 shows the level-spacing distribution functions for the ensembles of S_{ALS}^1 , S_{ALS}^2 , S_{MS}^1 , S_{MS}^2 , and S_0 by different symbols. We should remark that the distribution functions are normalized and the spacing s is rescaled by the mean level spacing Δ for each ensemble listed in Table I. The distribution function for S_0 is the same with that shown in Fig. 1. It is surprising that all distributions collapse onto a single universal curve which is identical to the conventional critical level-spacing distribution function for the two-dimensional symplectic class. This seems to conflict with the relation between the spectral correlation and wavefunction profiles. Naively, the function $P(s)$ for an ALS level-pair ensemble S_{ALS} would be more Poisson-like due to the localized nature of wavefunctions. Our numerical result indicates that ALS at the critical point do not affect the critical level-spacing distribution at all in spite of the fact that the probabil-

ity to find ALS at criticality is finite even in an infinite system. This implies that $P(s)$'s obtained by previous numerical works without paying attention to ALS represent the spectral correlation for typical critical states and can be used for judging the validity of theories for the critical level-spacing distribution based on the random matrix theory. In the next section, we will discuss the reason of this remarkable property of $P(s)$ at criticality. The inset of Fig. 2 shows mean level spacings for ALS and MS level-pair ensembles rescaled by the mean level spacing Δ_0 for the entire level-pair ensemble S_0 . The criteria Γ^* of level-pair ensembles means Γ_{ALS}^* for ALS level-pair ensembles and Γ_{MS}^* for MS ensembles. In the case of ALS level-pair ensembles (filled circles), the mean level spacing decreases from Δ_0 with increasing Γ_{ALS}^* , while for MS level-pair ensembles (open circles) it increases as decreasing Γ_{MS}^* . This implies that ALS level pairs mainly contribute to the level-spacing distribution in a small s region as demonstrated by Table I, which is consistent with the fact that the repulsive force between two adjacent levels corresponding to localized states is weak.

IV. DISCUSSIONS AND CONCLUSIONS

Let us consider the reason why the functional form of the critical level-spacing distribution $P(s)$ is not affected by ALS as shown in the previous section. To answer this question, it is important to examine carefully the spatial profile of ALS. Figure 3 shows squared amplitude distributions of an ALS ($\Gamma = 0.100$) at criticality, a typical MS ($\Gamma = 0.009$), and a localized state in the insulating phase ($W = 15.0$ and $E = 1.0$) of the SU(2) model of size $L = 120$. We see from the upper row of Fig. 3 that amplitudes of the ALS wavefunction [Fig. 3(a)] concentrate on a narrow region in the system, which resembles the usual localized state [Fig. 3(c)] in appearance and is in contrast to the MS wavefunction [Fig. 3(b)]. There exists, however, a crucial difference between profiles of ALS and truly localized states. The difference can be found in *tails* of wavefunctions. The lower row of Fig. 3 shows the gray-scale plots of the logarithm of squared amplitudes corresponding to the right above wavefunctions. For the truly localized state [Fig. 3(f)], amplitudes in logarithmic scale decrease with getting away from the localization

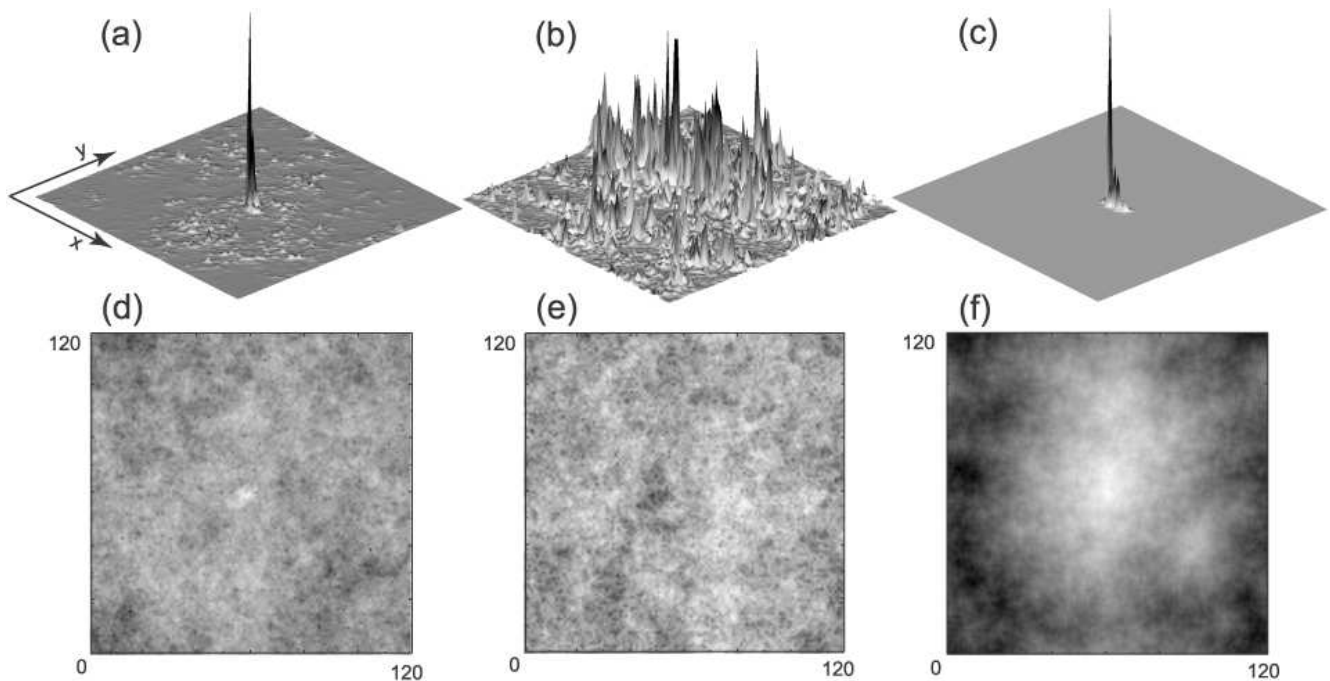


FIG. 3: Spatial profiles of an ALS [(a) and (d)], a MS [(b) and (e)], and a truly localized [(c) and (f)] wavefunctions. These wavefunctions are computed for the SU(2) model of size $L = 120$. The truly localized wavefunction [(c) and (f)] is an eigenstate of the system in the insulating phase ($W = 15.0$ and $E = 1.0$). Figures (d)-(f) represent the logarithm of squared amplitudes by gray-scale plots.

center (the center of the gray-scale plot), which means that the wavefunction decays exponentially. On the contrary, the ALS wavefunction does not possess such an exponential tail as demonstrated clearly in Fig. 3(d). It should be noted that the gray-scale range of Fig. 3(f) (10^{-36} to 10^{-1}) is much wider than that of Fig. 3(d) (10^{-10} to 10^{-2}). A remarkable feature of the ALS wavefunction is that the amplitude distribution away from the peak position of the ALS [the center of Fig. 3(d)] is quite similar to that shown in Fig. 3(e). This implies that amplitudes in the tail region of ALS distribute in a multifractal manner.

To confirm this perspective, we performed the multifractal analysis for the amplitude distribution only in the tail region of ALS. For this purpose, we have extracted a part of the eigenstate depicted by Fig. 3(a) within a 60×60 subsystem cut from the original system (120×120) so that the extracted eigenstate contains only a tail region of the whole eigenstate. (For cutting the subsystem, the original eigenstate has been appropriately shifted by taking the periodic boundary conditions into account.) In order to analyze its multifractal properties, we have renormalized the extracted wavefunction and calculated the box-measure correlation function $G_q(l, L, r)$ for $q = 1$, $L = L_s$, and $r = l$, where L_s is the size of the subsystem ($L_s = 60$). Figure 4 shows that the calculated $G_1(l, L_s, l)$ is proportional to l^{d+D_2} with $D_2 = 1.69 \pm 0.01$, where $D_2 = \tau(2)$ is the correlation dimension, while the correlation function $G_1(l, L, l)$ for

the whole wavefunction is not. This value of D_2 is very close to the value reported so far for typical multifractal wavefunctions belonging to this universality class.²⁶ This implies that tail regions of ALS exhibit the same multifractality with that of typical critical wavefunctions.^{41,42}

The tail structure of ALS gives a clue to understanding the behavior of $P(s)$ at criticality for the ALS level-pair ensemble S_{ALS} . Due to non-vanishing multifractal tails of ALS, quantum states belonging to adjacent ALS levels weakly couple each other through the overlap between wavefunctions in their tail region. As a consequence, we expect a repulsive force between these two ALS levels. The strength of the repulsive force is weaker than that for MS level pairs, because the average amplitude in the ALS tail region is small compared to the average of MS amplitudes. This explains a small mean level spacing for S_{ALS} as presented in Table I and the inset of Fig. 2. Since the spectral correlation is governed by overlaps of multifractal tails of ALS wavefunctions, it is reasonable that the critical level-spacing distribution for an ALS level-pair ensemble has the same functional form with $P(s)$ for MS level-pair ensembles. Multifractality in tails of ALS does not depend on the value of Γ_{ALS}^* . Therefore, the critical level-spacing distributions for the entire level-pair ensemble S_0 , the ALS ensemble S_{ALS} with any Γ_{ALS}^* , and the MS ensemble S_{MS} with any Γ_{MS}^* have the same profile, and all characteristics of level-spacing ensembles are absorbed by the mean level spacings.

The fact that the critical level-spacing distribution is

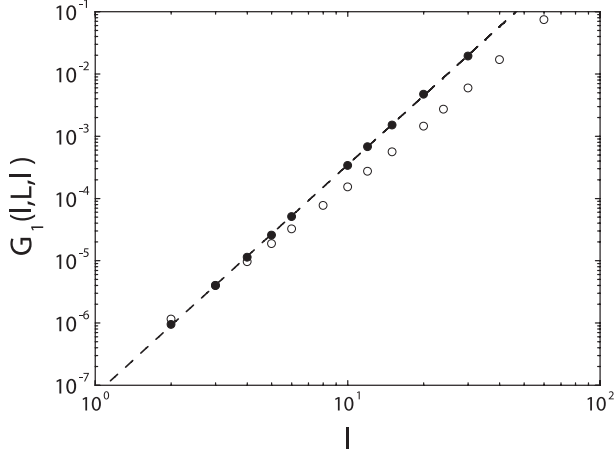


FIG. 4: Box-measure correlation functions $G_q(l, L, r)$ for $q = 1$ and $r = l$ for the whole eigenstate depicted by Fig. 3(a) (open circles, $L = 120$) and the part of the wavefunction containing a tail region cut from the original ALS wavefunction (filled circles, $L = L_s = 60$). Dashed line shows the least square fit for $G_1(l, L_s, l)$ for the extracted wavefunction.

invariant under changes of level-pair ensembles gives a condition for $P(s)$. If the ALS criteria Γ_{ALS}^* is equal to Γ_{MS}^* (say Γ^*), the entire level-pair ensemble S_0 can be decomposed into three ensembles S_{ALS} , S_{MS} and S_{mix} , where S_{mix} contains level pairs of ALS and MS, namely, $S_{\text{mix}}(\Gamma^*) = \{(\varepsilon, \varepsilon') : \Gamma > \Gamma^* \text{ and } \Gamma' < \Gamma^*\}$. These ensembles have no overlaps each other, i.e., $S_{\text{ALS}} \cap S_{\text{MS}} = S_{\text{MS}} \cap S_{\text{mix}} = S_{\text{mix}} \cap S_{\text{ALS}} = \phi$ (null set) and $S_0 = S_{\text{ALS}} \cup S_{\text{MS}} \cup S_{\text{mix}}$. In addition to $P(s)$'s for S_{ALS} and S_{MS} , we have also confirmed that the distribution $P(s)$ for S_{mix} has the same functional form with $P(s)$ for S_0 , S_{ALS} , or S_{MS} (see filled circles in Fig. 2). Thus, we have

$$P(s) = P_{\text{ALS}}(s) = P_{\text{MS}}(s) = P_{\text{mix}}(s), \quad (12)$$

for any value of Γ^* . Here, $P_x(s)$ is the critical distribution for S_x (x stands for the suffix “ALS”, “MS”, or “mix”). For $\Gamma_{\text{ALS}}^* = \Gamma_{\text{MS}}^*$, $P(s)$ can be expressed as a sum of contributions from S_{ALS} , S_{MS} , and S_{mix} :

$$P(s) = \tilde{P}_{\text{ALS}}(s) + \tilde{P}_{\text{MS}}(s) + \tilde{P}_{\text{mix}}(s), \quad (13)$$

where the distribution $\tilde{P}_x(s)$ is defined to be a function of the level spacing rescaled by the mean level spacing Δ_0 for S_0 (not S_x) and normalized as $\int \tilde{P}_x(s) ds = N_x/N_0$, where N_0 and N_x are the numbers of level pairs included in the ensembles S_0 and S_x , respectively. [$P_x(s)$ is a function of the spacing rescaled by Δ_x for S_x and normalized to unity.] Taking into account differences in the normalization conditions and the meanings of s , $\tilde{P}_x(s)$ is related to $P_x(s)$ as

$$\tilde{P}_x(s) = \frac{n_x}{\delta_x} P_x(s/\delta_x), \quad (14)$$

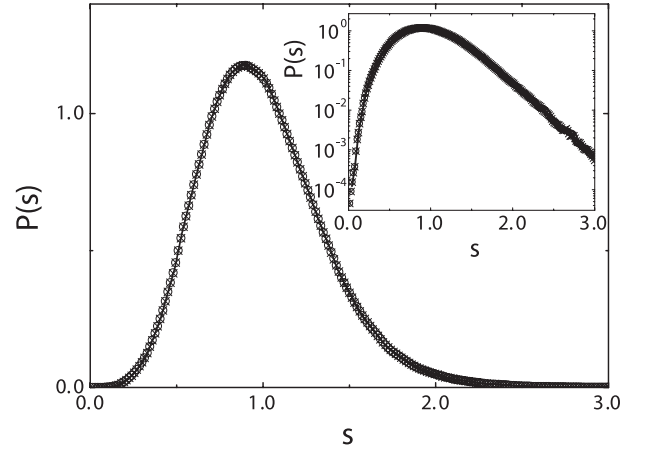


FIG. 5: Numerical confirmation of Eq. (15). Solid line represents the critical level-spacing distribution function calculated for the entire level-pair ensemble S_0 . Open circles and crosses are obtained from the right-hand side of Eq. (15) with $\Gamma^* = 0.01$ and 0.03 , respectively. The inset shows the same plots in a semilogarithmic scale.

where $n_x = N_x/N_0$ and $\delta_x = \Delta_x/\Delta_0$. Using Eqs. (12)–(14), we obtain

$$P(s) = \frac{n_{\text{ALS}}}{\delta_{\text{ALS}}} P(s/\delta_{\text{ALS}}) + \frac{n_{\text{MS}}}{\delta_{\text{MS}}} P(s/\delta_{\text{MS}}) + \frac{n_{\text{mix}}}{\delta_{\text{mix}}} P(s/\delta_{\text{mix}}). \quad (15)$$

Note that quantities n_x and δ_x depend on Γ^* . The critical level-spacing distribution function $P(s)$ should satisfy the above condition for any value of Γ^* .⁴³ Figure 5 shows numerically the validity of this condition. Data fabricated by using the right-hand side of Eq. (15) for $\Gamma^* = 0.01$ and 0.03 (symbols) agree quite well with the critical distribution itself (solid line).

We should note here that Eq. (15) is not consistent with the exponential behavior of the critical level-spacing distribution function in the large s limit, which is numerically observed in the inset of Fig. 1. Thus, Eq. (12) [or Eq. (15)] implies a *possibility* that the profile of $P(s)$ for $s \gg 1$ is not exactly exponential. For clarifying the asymptotic behavior of $P(s)$ for $s \gg 1$ or the validity of Eq. (12), further investigations are required.

In conclusion, we have studied the level-spacing distribution function $P(s)$ at the Anderson transition point of the two-dimensional $\text{SU}(2)$ model belonging to the symplectic class by paying attention to ALS. Since ALS at criticality exist with a finite probability even in the thermodynamic limit, quantities at the critical point might be influenced by ALS. Facts that ALS seem to have very different wavefunction profiles from typical MS ones and $P(s)$ is governed by spatial structures of wavefunctions intimate that the level-spacing distribution is greatly affected by ALS. To examine the influence of ALS to $P(s)$ at the critical point, we prepared numerically several

ALS (MS) level-pair ensembles which are constructed by pairs of ALS (MS) levels. Our remarkable result shows that level-spacing distributions for ALS level-pair ensembles coincide completely with those for MS and the entire ensembles, while the mean level spacing Δ for the ALS ensemble becomes smaller than Δ for the MS ensemble. Our findings imply that the spectral correlation for typical critical states can be evaluated even without eliminating ALS pairs from the original level-pair ensemble. Since ALS do not influence the function $P(s)$, the critical level-spacing distribution function can be understood by an analytical argument based on the random matrix theory in which ALS are not considered. We have also shown that the property of $P(s)$ insensitive to the existence of ALS is a consequence of multifractality in ALS tail structures. Furthermore, it has been pointed out that $P(s)$ should satisfy the condition derived from

the invariance of $P(s)$ under changes of level-pair ensembles. Although these results were obtained for the two-dimensional SU(2) model, we believe that the significant property of $P(s)$ is common in other universality classes.

Acknowledgments

We are grateful to T. Nakayama for helpful discussions. This work was supported in part by a Grant-in-Aid for Scientific Research from Japan Society for the Promotion of Science (No. 14540317). Numerical calculations in this work have been mainly performed on the facilities of the Supercomputer Center, Institute for Solid State Physics, University of Tokyo.

- ¹ L. P. Gorkov and G. M. Eliashberg, *Sov. Phys. JETP* **21**, 940 (1965).
- ² K. B. Efetov, *Adv. Phys.* **32**, 53 (1983).
- ³ B. L. Altshuler and B. I. Shklovskii, *Zh. Eksp. Tero. Fiz.* **91**, 220 (1986) [*Sov. Phys. JETP* **64**, 127 (1986)].
- ⁴ B. L. Altshuler, I. Kh. Zharekeshev, S. A. Kotochigova, and B. I. Shklovskii, *Zh. Eksp. Tero. Fiz.* **94**, 343 (1988) [*Sov. Phys. JETP* **63**, 625 (1988)].
- ⁵ M. L. Mehta, *Random Matrices*, 2nd ed. (Academic Press, New York, 1991).
- ⁶ S. N. Evangelou, *Phys. Rev. B* **39**, 12895 (1989).
- ⁷ E. Hofstetter and M. Schreiber, *Phys. Rev. B* **48**, 16979 (1993).
- ⁸ B. I. Shklovskii, B. Shapiro, B. R. Sears, P. Lambrianides, and H. B. Shore, *Phys. Rev. B* **47**, 11487 (1993).
- ⁹ Y. Ono, T. Ohtsuki, *J. Phys. Soc. Jpn.* **62**, 3813 (1993).
- ¹⁰ I. Kh. Zharekeshev, B. Kramer, *Phys. Rev. B* **51**, 17239 (1995).
- ¹¹ I. Varga, E. Hofstetter, J. Pipek, *Phys. Rev. Lett.* **82**, 4683 (1999).
- ¹² M. L. Ndawana, R. A. Römer, M. Schreiber, *Eur. Phys. J. B* **27**, 399 (2002).
- ¹³ H. Aoki, *J. Phys. C* **16**, L205 (1983); *Phys. Rev. B* **33**, 7310 (1986).
- ¹⁴ F. Wegner, *Z. Phys. B* **36**, 209 (1980).
- ¹⁵ For a recent review, see T. Nakayama and K. Yakubo, *Fractal Concepts in Condensed Matter Physics*. (Springer-Verlag, Berlin, 2003).
- ¹⁶ J. T. Chalker, V. E. Kravtsov and I. V. Lerner, *Pis'ma Zh. Eksp. Teor. Fiz.* **64**, 355 (1996) [*JETP Lett.* **64**, 386 (1996)].
- ¹⁷ A. G. Aronov, V. E. Kravtsov, and I. V. Lerner, *Pis'ma Zh. Eksp. Teor. Fiz.* **59**, 40 (1994) [*JETP Lett.* **59**, 39 (1994)].
- ¹⁸ V. E. Kravtsov, I. V. Lerner, B. L. Altshuler, and A. G. Aronov, *Phys. Rev. Lett.* **72**, 888 (1994).
- ¹⁹ L. Schweitzer and I. Kh. Zharekeshev, *J. Phys.: Condens. Matter* **7**, L377 (1995).
- ²⁰ S. N. Evangelou, *Phys. Rev. Lett.* **75**, 2550 (1995).
- ²¹ T. Ohtsuki and Y. Ono, *J. Phys. Soc. Jpn.* **64**, 4088 (1995).
- ²² T. Kawarabayashi, T. Ohtsuki, K. Slevin, and Y. Ono, *Phys. Rev. Lett.* **77**, 3593 (1996).
- ²³ I. Kh. Zharekeshev and B. Kramer, *Phys. Rev. Lett.* **79**, 717 (1997).
- ²⁴ V. E. Kravtsov and K. A. Muttalib, *Phys. Rev. Lett.* **79**, 1913 (1997).
- ²⁵ S. M. Nishigaki, *Phys. Rev. E* **58**, R6915 (1998); S. M. Nishigaki, *Phys. Rev. E* **59**, 2853 (1999).
- ²⁶ H. Obuse, K. Yakubo, *Phys. Rev. B* **69**, 125301 (2004).
- ²⁷ B. L. Altshuler, V. E. Kravtsov, and I. V. Lerner, *Pis'ma Zh. Eksp. Teor. Fiz.* **45**, 160 (1987) [*JETP Lett.* **45**, 199 (1987)].
- ²⁸ For a comprehensive review, see A. D. Mirlin, *Phy. Rep.* **326**, 259 (2000).
- ²⁹ B. A. Muzykantskii and D. E. Khmelnitskii, *Phys. Rev. B* **51**, 5480 (1995).
- ³⁰ V. I. Fal'ko and K. B. Efetov, *Phys. Rev. B* **52**, 17413 (1995).
- ³¹ V. Uski, B. Mehlig, R. A. Römer, and M. Schreiber, *Phys. Rev. B* **62**, R7699 (2000); V. Uski, B. Mehlig, and M. Schreiber, *Phys. Rev. B* **66**, 233104 (2002).
- ³² B. K. Nikolić, *Phys. Rev. B* **64**, 14203 (2001); B. K. Nikolić, *Phys. Rev. B* **65**, 012201 (2001); B. K. Nikolić and V. Z. Cerovski, *Eur. Phys. J. B* **30**, 227 (2002).
- ³³ T. Kottos, A. Ossipov, and T. Geisel, *Phys. Rev. E* **68**, 066215 (2003); A. Ossipov, T. Kottos, and T. Geisel, *Eur. Phys. Lett.* **62**, 719 (2003).
- ³⁴ It has been pointed out that values of multifractal exponents depend on averaging procedures in a random Dirac fermion model. [H. E. Castillo, C. C. Chamon, E. Fradkin, P. M. Goldbart, and C. Mudry, *Phys. Rev. B* **56**, 10668 (1997)].
- ³⁵ Y. Asada, K. Slevin, and T. Ohtsuki, *Phys. Rev. Lett.* **89**, 256601 (2002).
- ³⁶ M. Janssen, *Int. J. Mod. Phys. B* **8**, 943 (1994).
- ³⁷ A. Kyralla, *Theoretical Physics: Applications of Vectors, Matrices, Tensors and Quaternions* (Philadelphia, London, 1967).
- ³⁸ T. Nakayama and K. Yakubo, *Phys. Rep.* **349**, 239 (2001).
- ³⁹ Details of the forced oscillator method for quaternion-real matrices will be published elsewhere.
- ⁴⁰ T. Ando, *Phys. Rev. B* **40**, 5325 (1989).
- ⁴¹ The power law behavior in a ALS tail region has been

predicted by Ref. 30 in a metallic phase of two-dimensional symplectic systems.

- ⁴² There exist another type of ALS in the metallic phase, which are exponentially localized. [V. M. Apalkov, M. E. Raikh, and B. Shapiro, Phys. Rev. Lett. **89**, 16802 (2002); V. M. Apalkov, M. E. Raikh, and B. Shapiro, Phys. Rev. Lett. **89**, 126601 (2002); V. M. Apalkov, M. E. Raikh, and B. Shapiro, Phys. Rev. Lett. **92** 066601 (2004)]. However,

we do not find such exponentially localized states at the critical point.

- ⁴³ Three terms in the right-hand side of Eq. (15) are single-peak functions with different peak positions. This does not mean that the sum of these three terms has three peaks, because the peak positions are very close each other.